



## EDS

# Application example for the XFlash® FlatQUAD: High vacuum and low beam current analysis

Application Note # EDS-12

### Introduction

Non-destructive sample analysis with high spatial resolution can be very difficult to accomplish using conventional EDS detectors as sample surface charging, electron beam damage and shading effects by topography are common problems in scanning electron microscopy. The BRUKER XFlash® FlatQUAD silicon drift detector (SDD) overcomes these limitations. The special geometry with an annular arrangement of detector elements offers a very high solid angle [1].

The XFlash® FlatQUAD detector allows the use of ultra-low beam currents and the investigation of samples with complex topography as demonstrated on two meteorite fall samples.

The Mocs historic meteorite fell on February 2, 1882 in Hungary [2]. The historically cut sample (Figure 1 left) was stored at Naturhistorisches Museum Wien (Natural History Museum, Vienna, Austria) for the last century. Studies recently carried out with the Bruker M4 TORNADO benchtop Micro-XRF spectrometer revealed an unexpected lead enrichment

along cracks (Figure 1 right). This finding led to a detailed analysis using the XFlash® FlatQUAD detector. The second study was carried out on a piece of the Tissint Martian meteorite that fell in Morocco on July 18, 2011 [3]. Tissint is only the fifth Martian meteorite that people have witnessed falling to Earth, the last time such an event happened was in 1962. Thus, the scientific value of these unique meteorites excludes sample preparation.

### Method

The XFlash® FlatQUAD is an annular SDD arrangement which is placed between the pole piece and the sample. This special geometry is ideal for the analysis of topographically complex samples. Shadowing effects are minimized by collecting X-rays from four separate detector segments with high take-off angles. Additionally, the large solid angle of up to 1.1 sr enables EDS analysis with reasonable count rates using ultra-low beam currents of <10 pA. As a result, the charging of nonconductive samples under

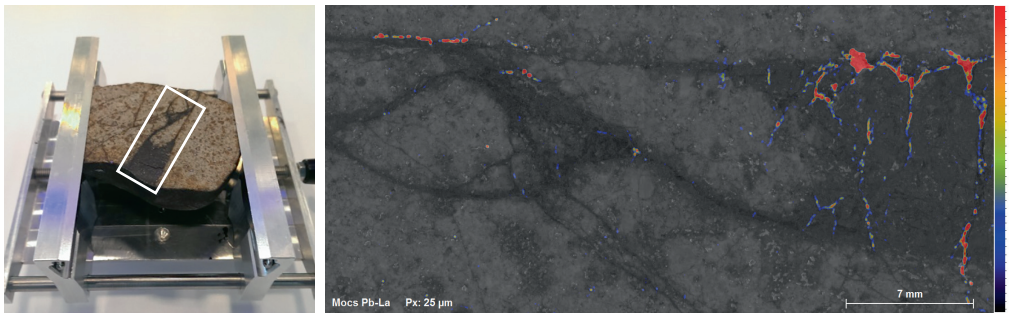


**Figure 1**  
Mocs historic meteorite; (left) Photograph of the cut sample. The rectangle shows the area analyzed with micro-XRF. For EDS analysis the specimen was mounted on a sample holder and analyzed without carbon coating. (right) Video image overlaid with the micro-XRF map of the lead La X-ray line (1472 pixel x 676 pixel, 25 μm pixel size, 33 min acquisition time) showing lead enrichment along cracks.

high vacuum is minimized. This approach therefore enables non-destructive EDS analysis of sensitive topographic samples, as sample preparation like polishing and carbon coating is not required.

For this study, low accelerating voltages (< 6 kV, see also Table 1) were used to examine fine

structures. This decreases the interaction volume for electron trajectories and the emitted X-rays, as shown in Figure 2.

The peak overlaps of low to intermediate energy X-ray lines (Figure 3) were deconvolved using an extended atomic database [4] and an automatic routine.

	<b>Mocs (overview)</b>	<b>Mocs (crack)</b>	<b>Tissint</b>
Accelerating voltage / kV	6	6	4
T Beam current / pA	< 10	< 10	< 10
Input count rate / kcps	2.9	2.4	1.8
Map resolution / pixels <sup>2</sup>	800 x 600	1600 x 1200	1280 x 853
Pixel resolution	2 μm	130 nm	55 nm
Acquisition time	47 min	15 h	13 h

**Table 1**  
Measurement conditions used for acquiring the maps discussed in this report. Due to the specific geometry of the annular XFlash<sup>®</sup> FlatQUAD, the input count rate of the map with low topography in the crack of the Mocs meteorite is just slightly lower than that of the overview map.

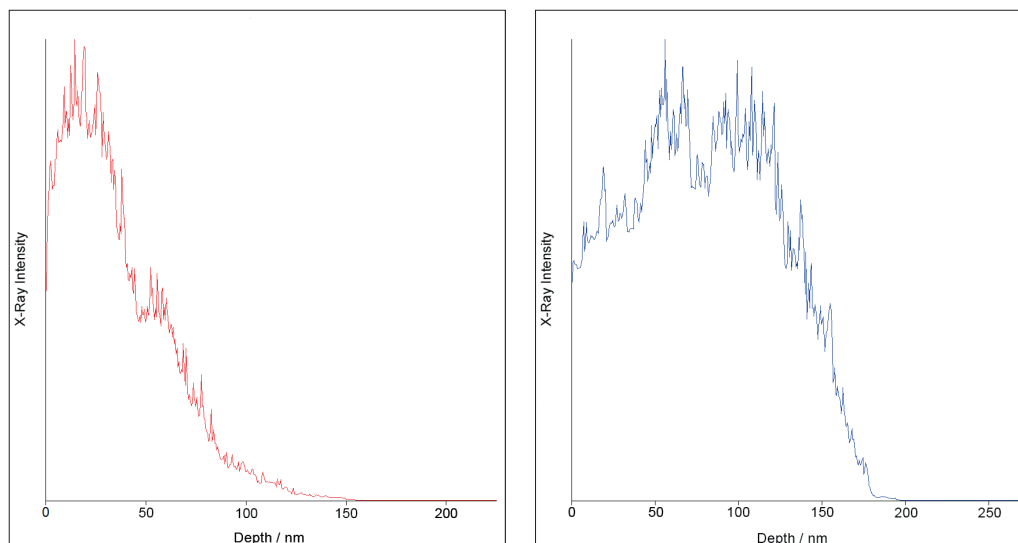


**Figure 2**  
The X-ray excitation depth functions display the intensity of emitted X-rays depending on their depth in the sample. The highest X-ray intensities are emitted mainly from a depth ~50 nm for lead M at 6 kV (red graph) and ~150 nm for carbon K at 4 kV (blue graph). It shows that the spatial resolution for EDS X-ray analysis can be significantly enhanced by using low accelerating voltages.

In case of the Mocs meteorite, a region of interest was identified first with an overview map within just 47 minutes. A second map was carried out at high resolution overnight using 6 kV and 130 nm pixel size. The Tissint Martian meteorite was analyzed overnight using 4 kV and 55 nm pixel size.

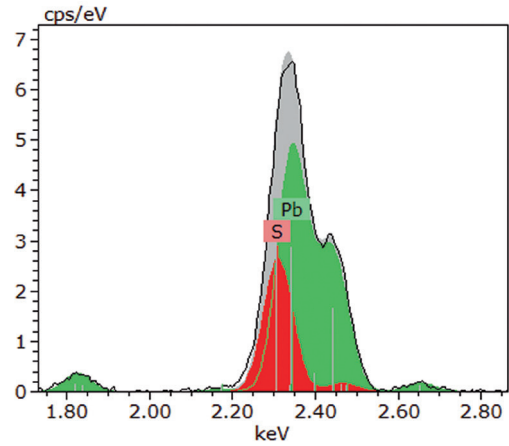


**Figure 3**  
Deconvolution result of Pb (green) and S (red) showing the separation of the overlapping element lines lead M and sulfur K

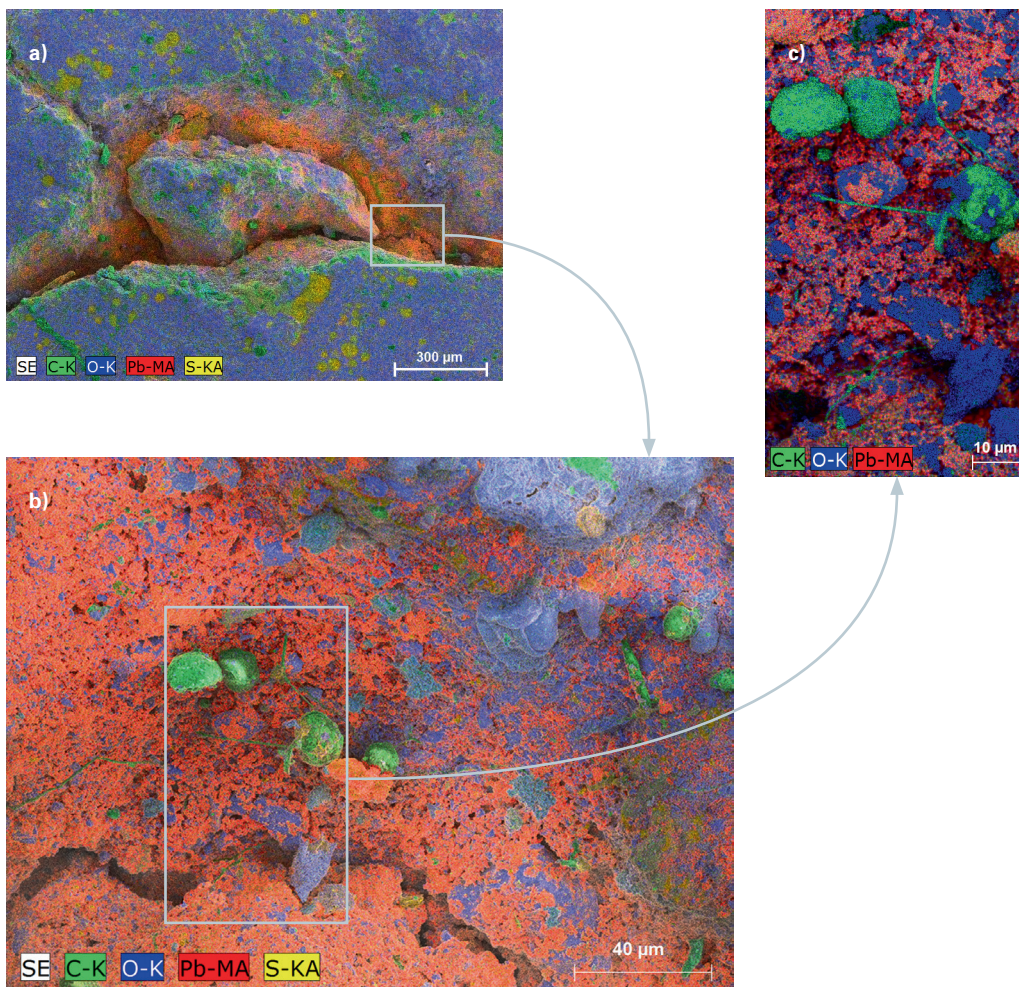


**Figure 4**  
Mocs historic meteorite; Element maps of integrated peak intensities.  
(a) The composite map overlaid with the SE micrograph reveals lead contamination from the historical cutting process.  
(b) The composite map of the rectangular area in (a) overlaid with the SE micrograph shows that lead and soot is deposited on silicates.  
(c) Image detail of the area shown in (b) without SE micrograph. It documents that carbon features < 300 nm in size (green filaments) can be made visible under high vacuum using low HV and ultra-low beam currents.

## Results

Figure 4a shows the area of the overview map of the Mocs meteorite. It indicates an enrichment of lead in cracks, most likely caused by discs containing lead that were used as cutting tools in the past. Sufficient

data quality allows deconvolution of overlapping element lines (Pb M, S K) and therefore the distinction of lead contamination and sulfide minerals contained in the meteorite material. EDS analysis at high spatial resolution (Figures 4 b and c) shows the deposition of lead on silicates and sulfides. Spherical

carbon particles and filaments with sizes < 300 nm are a sign of surface contamination with soot resulting from heating the Natural History Museum of Vienna with coal-fired furnaces during the last century. Figure 5 shows a portion of the Tissint Martian meteorite. The mapped area reveals a thin coating and local enrichment of carbon and nitrogen which are associated with topographic features.

## Conclusion

Although meteorite samples are less common in the everyday work of the analyst, they are a good example to demonstrate the capabilities of the novel detector concept of the annular XFlash® FlatQUAD as they present not only one but a combination of several analytical obstacles for EDS with a standard single-chip detector.

Element analysis at low accelerating voltages and low beam current provides high spatial resolution and high detection sensitivity without the necessity of applying a conductive coating or working in low vacuum. Compared to low vacuum analysis, this approach avoids beam skirting effects where the lateral resolution for EDS X-ray analysis is affected due to the collision of electrons with atoms / molecules of gas.

In addition hydrocarbon contamination is dramatically reduced, which provides the possibility to analyze beam sensitive or precious specimens in a close to natural state without preparation and to study small scale structures. This includes carbon containing surface layers (Tissint) which would otherwise be seriously affected by the above mentioned carbon contamination.

In summary the use of the XFlash® FlatQUAD detector supports new analytical approaches for various fields, especially biological and cultural heritage sciences and nanoparticle characterization.

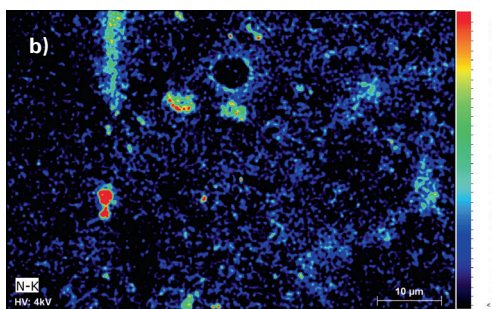
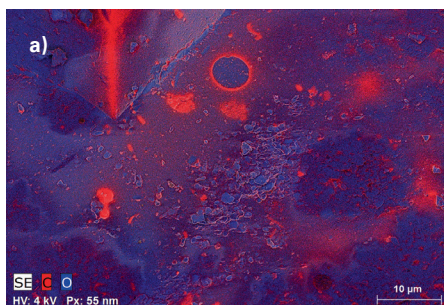


**Figure 5**

Tissint Martian meteorite; (a) the composite map of carbon and oxygen overlaid with the SE micrograph shows a thin coating and local enrichment of carbon on a silicate surface. (b) The distribution of nitrogen with low intensities can be made visible by using a false color display of the according map.

## References

- [1] Technical Information Note EDS #1: Solid angle and EDS detector area. Background information and solid angle optimization. [https://www.bruker.com/fileadmin/user\\_upload/8-PDF-Docs/XrayDiffraction\\_ElementalAnalysis/Microanalysis\\_EBSD/InfoNotes/info\\_note\\_01\\_lowres.pdf](https://www.bruker.com/fileadmin/user_upload/8-PDF-Docs/XrayDiffraction_ElementalAnalysis/Microanalysis_EBSD/InfoNotes/info_note_01_lowres.pdf)
- [2] Miura, Y., Iancu, G., Yanai, K., Haramura, H., (1995): Proceedings NIPR Symposium of Antarctic Meteorites, Vol. 8, 153-166
- [3] Aoudjehane, H. C. et. al, (2012): Tissint Martian Meteorite: A Fresh Look at the Interior, Surface, and Atmosphere of Mars, Science, Vol. 338, Issue 6108, 785-788
- [4] Aßmann, A. and Wendt, M., (2003): The identification of soft X-ray lines: Spectrochimica Acta Part B, Vol. 58, 711-716.

## Acknowledgements

Dr. Ludovic Ferrière (Naturhistorisches Museum Wien, Austria) and Dr. Caroline Smith (Earth Sciences Department, Mineral and Planetary Sciences Division, Natural History Museum of London, United Kingdom) for providing the sample.

Dr. A. D. Ball, Dr. C. Jones, Dr. A. T. Kearsley (Science Facilities, Natural History Museum, London, United Kingdom) for sample analysis.

## Authors

Dr. Tobias Salge, Senior Application Scientist EDS, Bruker Nano GmbH

Dr. Roald Tagle, Senior Application Scientist Micro-XRF, Bruker Nano GmbH

## Bruker Nano Analytics

Headquarters Berlin · Germany  
info.bna@bruker.com

[www.bruker.com/quantax-eds-for-sem](http://www.bruker.com/quantax-eds-for-sem)

